J|A|C|S COMMUNICATIONS

Published on Web 10/26/2010

Molecular Stress Relief through a Force-Induced Irreversible Extension in Polymer Contour Length

Dong Wu, Jeremy M. Lenhardt, Ashley L. Black, Boris B. Akhremitchev,*,[+] and Stephen L. Craig*

Department of Chemistry and Center for Biologically Inspired Materials and Material Systems, Duke University, Durham, North Carolina 27708-0346, United States

Received September 17, 2010; E-mail: bakhremitchev@fit.edu; stephen.craig@duke.edu

Abstract: Single-molecule force spectroscopy is used to observe the irreversible extension of a *gem*-dibromocyclopropane (*g*DBC)-functionalized polybutadiene under tension, a process akin to polymer necking at a single-molecule level. The extension of close to 28% in the contour length of the polymer backbone occurs at roughly 1.2 nN (tip velocity of 3 μm/s) and is attributed to the force-induced isomerization of the *g*DBCs into 2,3-dibromoalkenes. The rearrangement represents a possible new mechanism for localized stress relief in polymers and polymer networks under load, and the quantification of the force dependency provides a benchmark value for further studies of mechanically triggered chemistry in bulk polymers.

Localized stress concentrations in polymers under load are often responsible for material failure. The challenge of stress concentration is a persistent one, because it is difficult, if not impossible, to control polymer topology in such a way that the load is distributed evenly among individual polymer molecules. One attractive, albeit speculative, strategy in polymer design, therefore, is to incorporate along the polymer backbone stress-responsive mechanophores that sense local stress and trigger chemistry that remodels the at-risk chain segments in a productive manner.[1,2] Here we report the direct observation, by single-molecule force spectroscopy (SMFS), of force-accelerated, covalent polymer extensions of up to ~28% in the contour length of active, stress-bearing *gem*-dibromocyclopropane (*g*DBC) polymer chain segments. The localized "stress relief" [3] allows the polymer to survive strains that are typically catastrophic. The SMFS measurements further allow the force dependence of the *g*DBC ring opening to be quantified, providing a foundation for future studies of force-induced chemistry in the bulk.

The addition of dibromocarbene to *cis*-polybutadiene (PB) under phase-transfer conditions yielded *g*DBC-functionalized polymers with 36%, 68%, and >98% *g*DBC content by ^{1}H NMR. THF solutions of *g*DBC-PB were dried on silicon substrates, which were then placed into an atomic force microscope (AFM) flow cell and immersed in dioxane:acetonitrile (5:1). Subsequent contact and withdrawal of the AFM tip at velocities of 3 μm s^{-1} revealed the attachment and extension of polymers adhered to both the tip and the substrate.

The majority of the polymers detached at low (<a few hundred piconewtons) forces, but a few remained attached at forces in excess of 1 nN. Without exception, polymers that remained adhered at a force of ca. 1.2 nN underwent a transition at that force, as revealed by a plateau in the force−extension curve (Figure 1). The transition is indicative of structural change that results in extension of the polymer backbone, as observed previously, for example, in proline-rich polypeptides[4] or double-stranded DNA.[5] Here, the polymer extension is attributed to the conversion of the *g*DBCs into the corresponding 2,3-dibromoalkenes—a reaction class known to be accelerated by tension[6] (Figure 1). The observed extensions are consistent with this interpretation, as the length of the plateau is proportional to *g*DBC content: the 36% *g*DBC-PB copolymer extends to 1.11 times its initial contour length, while the 68% *g*DBC polymers lengthen on average by a factor of 1.20 and the fully functionalized polymers by a factor of 1.28 (Table 1). The absolute magnitudes of the extensions are consistent with the expected rearrangement. Computational modeling gives computed changes in respective contour lengths of 1.10, 1.19, and 1.28 (Supporting Information).

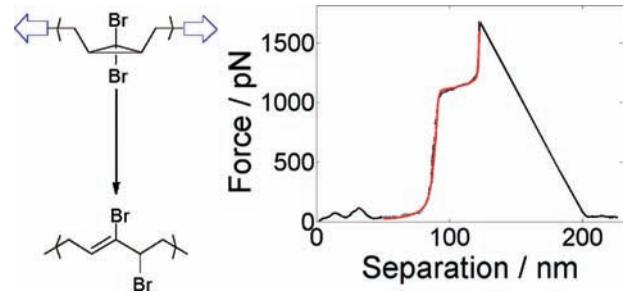

Figure 1. Single-molecule force spectroscopy was used to monitor the electrocyclic ring opening of *g*DBC. Force versus extension curves were fit to both the cusp and Bell−Evans models (BE fit above, red line, 100% *g*DBC, $\Delta x^{\ddagger} = 1.08$ Å, 34% extension).

Table 1. Parameters Obtained from Fits to SMFS Data of *g*DBC-Functionalized Polybutadiene

		$\Delta x^{\ddagger}$/Å		
entry	*g*DBC content/%[a]	BE	cusp	L_f/L_i[b]
1	>98	1.08	1.32	1.34
2	>98	1.23	1.50	1.23
3	68	0.93	1.12	1.21
4	68	0.99	1.20	1.19
5	36	1.03	1.24	1.11

[a] Determined by ^{1}H NMR. [b] Ratio of final to initial contour length.

The transition is irreversible, as revealed by hysteresis in the fortuitous capture and relaxation of a partially extended polymer; the contour length of the polymer is seen to have increased in the subsequent retraction cycle (see Supporting Information). The *g*DBC mechanophores therefore complement mechanophores that contract in response to transient extension.[7] The polymer extension enables the polymer to continue to actively support a load at strains that would otherwise result in catastrophic failure. In a conventional, mechanically inactive polymer, the force increases dramatically with strain as the polymer is stretched to its fully extended contour length

[+] Present address: Department of Chemistry, Florida Institute of Technology, Melbourne, FL 32901.

10.1021/ja108429h

and then beyond as bond angles are deformed. Once a polymer reaches a restoring force of 1 nN, for example, an additional extension of just a few percent would typically result in tensions of several nanonewtons and concomitant chain scission. In the *g*DBC polymers, however, an additional strain of ~28% is accommodated. Because the transition occurs at the high forces that occur near failure strains, it provides a dramatic increase in toughness (net energy absorbed, or area under the curve) at the single-molecule level due to covalent bond rearrangements: more than 10^4 kJ mol^{-1} for the polymer shown in Figure 1.

Kinetic data were extracted from the SMFS curves by assuming the independent conversion of each *g*DBC monomer into a 2,3-dibromoalkene. Unlike many SMFS experiments, which often record a single event, each force curve here captures hundreds or thousands of events and provides a statistically significant sample for data analysis—an advantage found in the polyprotein technique described by Fernandez and co-workers.[8] The presence of many events allows the rate of ring opening at the plateau force to be extracted directly from the time scale over which the extension occurs, by extending previous model-free rate-vs-force analyses.[9,10] Here, the calculated rate constant for *g*DBC ring opening is ~10^2 s^{-1} at 1.2 nN. The force-coupled ring opening is roughly 10^{13} times faster than the force-free reaction, for which a rate constant $k_0 = 3 \times 10^{-11}$ s^{-1} was obtained from conventional reaction-rate theory, using a literature value (both theoretical[11] and experimental[12]) of $\Delta G^{\ddagger} = 32$ kcal mol^{-1} for the force-free activation energy.

We further fit the force curves by treating the rate as a function of force with the Bell−Evans (BE) theory (eq 1),

$$k(F) = k_0 \exp(-F\Delta x^{\ddagger}/k_B T) \qquad (1)$$

and coupling eq 1 to freely jointed chain models of polymer extension (Figure 1).[13−15] The fits provide an apparent value of $\Delta x^{\ddagger}$ which quantifies the force dependency of the reaction and is classically interpreted as the extension of the *g*DBC in the transition state that is coupled to the applied tension (Table 1). Measurements were obtained on polymers of three different *g*DBC contents, on different days, using four different AFM tips. They therefore capture the day-to-day variations due to calibration or sample preparation. Fits to five different force curves give consistent values for $\Delta x^{\ddagger}$ of 1.05 ± 0.11 Å. We point out that these data comprise every force curve for which the profile is consistent with that of an isolated single-chain extension. Some force curves showed plateaus at the same 1.2 nN force but were excluded from the kinetic analysis because they showed signatures of non-single-extension behavior (e.g., multiple simultaneous polymer extensions, loop formation; see Supporting Information).

It is tempting to try to assign specific molecular significance to the derived $\Delta x^{\ddagger}$, but it is not clear, either theoretically or empirically, that the fitting parameter should represent a simple internal coordinate of the reactant. The derived $\Delta x^{\ddagger}$ values, for example, are far larger than the extension of the scissile $C_1-C_{1'}$ bond (0.67 Å) in the transition state for the dimethyl *g*DBC ring opening calculated previously by Faza et al. (Figure 2a).[11] The C−C distance associated with the scissile bond is clearly not the correct reaction coordinate by which to describe mechanical activation—a perspective proposed in the context of other electrocyclic ring opening reactions.[16−18] Because the outward rotation of the attached methylenes is necessarily coupled to the ring opening, the $C_2-C_{2'}$ separation (Figure 2a) is another reasonable choice for relevant molecular parameter, and one that has proven effective for interpreting the internal force dependence of the electrocyclic ring opening of cyclobutene in strained macrocycles.[16] The calculated

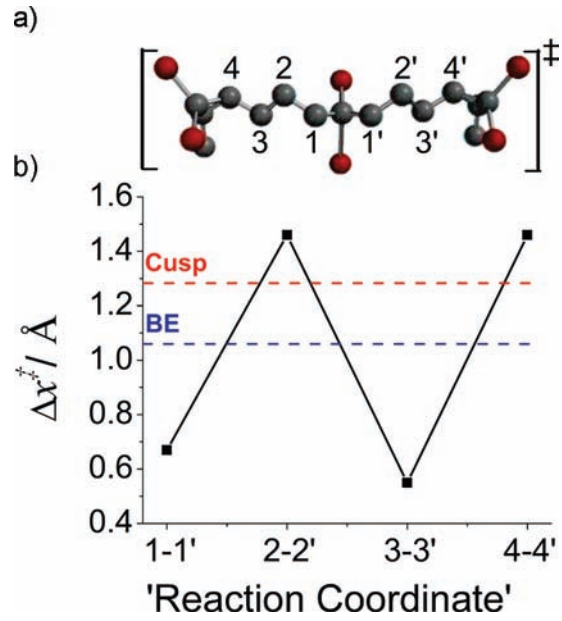

Figure 2. (a) Transition-state structure for the *g*DBC ring-opening reaction, with additional *g*DBC monomers added to either side and allowed to relax computationally (AM1, implemented in Spartan). (b) Calculated distances from the ground- (see Supporting Information) to transition-state structure as a function of the $C_x-C_{x'}$ position, beginning at the scissile bond in the *g*DBC. Dotted lines denote the $\Delta x^{\ddagger}$ values obtained from BE and cusp model fits.

increase in $C_2-C_{2'}$ distance at the transition state (1.46 Å), however, is greater than the experimentally derived $\Delta x^{\ddagger}$, and values change in an alternating fashion for the $C_3-C_{3'}$ (0.55 Å) and $C_4-C_{4'}$ (1.46 Å) separations (Figure 2b). Similar even−odd alternation has been recently calculated for the ring opening of benzocyclobutenes mechanically coupled through tethered alkyl groups.[19]

None of the aforementioned reaction coordinates provide a value that agrees with that derived from the experiment. One reason for the difference might be the assumption within the BE theory that $\Delta x^{\ddagger}$ does not change with increasing force (i.e., reaction potential energy is linear with respect to x along the reaction coordinate). Previous studies found this assumption to be reasonable for electrocyclic ring opening of cyclobutene,[16] but to test possible contributions we nonetheless fit the force curves assuming an inflection in the potential energy surface as reflected by the cusp model.[20] Because of the inflection in the potential energy surface, the effective $\Delta x^{\ddagger}$ gets shorter as the force increases: the ground state is extended, and the position of the transition state drifts toward shorter conformations. Thus, the cusp value for the force-free $\Delta x^{\ddagger}$ derived from a given force curve is greater than that associated with a BE fit to the same curve. The derived $\Delta x^{\ddagger}$ value of 1.28 ± 0.14 Å (Table 1) is closer to, but still differs from, the calculated $C_2-C_{2'}$ (or $C_4-C_{4'}$) separation. We point out that (1) these analyses are anchored to the calculations of Faza et al.[11] and (2) different functional relationships between k and F would, of course, lead to different values of $\Delta x^{\ddagger}$.

In addition, the effective value of $\Delta x^{\ddagger}$ might reflect coupling between the reaction and the motions of atoms along the polymer backbone. The odd/even pattern in calculated C−C extension, for example, is consistent with Ribas-Arino et al.'s conclusion[19] that the polymeric attachment cannot be ignored in the treatment of mechanochemical coupling. The effects of tensile forces applied to the ends of polymers[21−24] might therefore differ from those in, for example, strained macrocycles,[16] for which the applied force is calculated at very specific atomic positions. These differences

might persist even in situations where the force-free reactivities are otherwise quite similar. Assessing the relative contributions of polymer architecture and the shape of the reaction potential energy surface represents a challenge for future theoretical work.

Because they are direct, the SMFS measurements provide a valuable foundation for understanding mechanophore activity in a polymer materials context. The irreversible extension of the *g*DBCs occurs on the time scale of 10^{-2} s at 1.2 nN—a benchmark value that can be used to assess molecular force distributions in the solid state. From a properties viewpoint, the isolated polymers completely remodel under tension prior to failure, and so these polymers withstand strains well in excess of those tolerated by conventional covalent polymer backbones. In that respect, the covalent processes described here are reminiscent of the disruption of sacrificial bonds in biological[25] and synthetic[26] systems, but with irreversible transitions that are localized at the level of individual monomers. We hypothesize that, once optimized, the covalent stress-relief strategy can be used to distribute load evenly among stress-bearing segments, thereby remodeling polymer networks in response to their mechanical environment for maximum strength and toughness.

Acknowledgment. This material is based on work supported by the U.S. Army Research Laboratory and the Army Research Office under grant number W911NF-07-1-0409. J.M.L. is supported by the ACS Division of Organic Chemistry Schering-Plough Fellowship. We thank D. Chang for helpful discussions.

Supporting Information Available: Synthesis and characterization of polymers, details of SMFS procedure and analysis, and examples of force curves excluded from kinetic analysis. This material is available free of charge via the Internet at http://pubs.acs.org.

References

(1) Davis, D. A.; Hamilton, A.; Yang, J.; Cremar, L. D.; Van Gough, D.; Potisek, S. L.; Ong, M. T.; Braun, P. V.; Martinez, T. J.; White, S. R.; Moore, J. S.; Sottos, N. R. *Nature* **2009**, *459*, 68–72.
(2) Piermattei, A.; Karthikeyan, S.; Sijbesma, R. P. *Nature Chem.* **2009**, *1*, 133–137.
(3) Mechanical stress is typically defined in the context of continuum mechanics and not for single molecules. Our use of the term here should be interpreted as being descriptive only.
(4) Valiaev, A.; Lim, D. W.; Oas, T. G.; Chilkoti, A.; Zauscher, S. *J. Am. Chem. Soc.* **2007**, *129*, 6491–6497.
(5) Bustamante, C.; Smith, S. B.; Liphardt, J.; Smith, D. *Curr. Opin. Struct. Biol.* **2000**, *10*, 279–285.
(6) Lenhardt, J. M.; Black, A. L.; Craig, S. L. *J. Am. Chem. Soc.* **2009**, *131*, 10818–10819.
(7) Lenhardt, J. M.; Ong, M. T.; Choe, R.; Evenhuis, C. R.; Martinez, T. J.; Craig, S. L. *Science* **2010**, *329*, 1057–1060.
(8) Koti Ainavarapu, S. R.; Wiita, A. P.; Dougan, L.; Uggerud, E.; Fernandez, J. M. *J. Am. Chem. Soc.* **2008**, *130*, 6479–6487.
(9) Serpe, M. J.; Kersey, F. R.; Whitehead, J. R.; Wilson, S. M.; Clark, R. L.; Craig, S. L. *J. Phys. Chem. C* **2008**, *112*, 19163–19167.
(10) Oberbarnscheidt, L.; Janissen, R.; Oesterhelt, F. *Biophys. J.* **2009**, *97*, L19–L21.
(11) Faza, O. N.; López, C. S.; Álvarez, R.; de Lera, Á. R. *J. Org. Chem.* **2004**, *69*, 9002–9010.
(12) Duffey, D. C.; Minyard, J. P.; Lane, R. H. *J. Org. Chem.* **1966**, *31*, 3865–3867.
(13) Evans, E.; Ritchie, K. *Biophys. J.* **1997**, *72*, 1541–1555.
(14) Evans, E. *Annu. Rev. Biophys. Biomol. Struct.* **2001**, *30*, 105–128.
(15) Ray, C.; Brown, J. R.; Akhremitchev, B. B. *J. Phys. Chem. B* **2007**, *111*, 1963–1974.
(16) Huang, Z.; Yang, Q.-Z.; Khvostichenko, D.; Kucharski, T. J.; Chen, J.; Boulatov, R. *J. Am. Chem. Soc.* **2009**, *131*, 1407–1409.
(17) Yang, Q.-Z.; Huang, Z.; Kucharski, T. J.; Khvostichenko, D.; Chen, J.; Boulatov, R. *Nature Nanotechnol.* **2009**, *4*, 302–306.
(18) Hickenboth, C. R.; Moore, J. S.; White, S. R.; Sottos, N. R.; Baudry, J.; Wilson, S. R. *Nature* **2007**, *446*, 423–427.
(19) Ribas-Arino, J.; Shiga, M.; Marx, D. *J. Am. Chem. Soc.* **2010**, *132*, 10609–10614.
(20) Hummer, G.; Szabo, A. *Biophys. J.* **2003**, *85*, 5–15.
(21) Kersey, F. R.; Yount, W. C.; Craig, S. L. *J. Am. Chem. Soc.* **2006**, *128*, 3886–3887.
(22) Kryger, M. J.; Ong, M. T.; Odom, S. A.; Sottos, N. R.; White, S. R.; Martinez, T. J.; Moore, J. S. *J. Am. Chem. Soc.* **2010**, *132*, 4558–4559.
(23) Wiggins, K. M.; Hudnall, T. W.; Shen, Q.; Kryger, M. J.; Moore, J. S.; Bielawski, C. W. *J. Am. Chem. Soc.* **2010**, *132*, 3256–3257.
(24) Potisek, S. L.; Davis, D. A.; Sottos, N. R.; White, S. R.; Moore, J. S. *J. Am. Chem. Soc.* **2007**, *129*, 13808–13809.
(25) Fantner, G. E.; Hassenkam, T.; Kindt, J. H.; Weaver, J. C.; Birkedal, H.; Pechenik, L.; Cutroni, J. A.; Cidade, G. A. G.; Stucky, G. D.; Morse, D. E.; Hansma, P. K. *Nat. Mater.* **2005**, *4*, 612–616.
(26) Kushner, A. M.; Gabuchian, V.; Johnson, E. G.; Guan, Z. *J. Am. Chem. Soc.* **2007**, *129*, 14110–14111.

JA108429H